Genetic variation in *HIF1A* is associated with smoldering inflammation and disease progression in Multiple Sclerosis

Giordano A, et al.

Supplement

Table of contents

SUPPLEMENTARY METHODS

Genetic association study

Cohorts for the genetic study

For the genetic association study, we compared RR-MS patients, who did not experience disease progression for the first 20 years from disease onset and with an Expanded Disability Status Scale (EDSS) score ≤ 3.5 at last follow-up, with SP-MS patients, who had confirmed disease progression within 20 years from disease onset and EDSS ≥ 4.0 at last follow-up. Starting from a large cohort of MS patients with available whole-genome genotype data at the Laboratory of Human Genetics of Neurological Disorders at the San Raffaele Scientific Institute (ITA), we identified 772 patients with definite diagnosis of MS according to 2017 revised criteria[1], who fulfilled the above-mentioned inclusion criteria for RR-MS (n=406) or SP-MS (n=366), and underwent quality control for the genetic study. To replicate significant associations emerging from the ITA cohort study, we took advantage of a large Swedish nationwide cohort (SWE) gathered at the Karolinska Institutet (Stockholm, Sweden). The subjects of the SWE cohort were part of the National Swedish MS Registry. Clinical information and blood samples for genotyping were gathered and managed at the Karolinska Institutet. In the SWE cohort, a total of 2,062 patients with RR-MS (n=863) and SP-MS (n=1,199) were included, who fulfilled the same criteria used for the discovery cohort.

Genotype imputation and quality control in the ITA cohort

As mentioned, a large cohort of MS patients with available whole-genome genotype information was available at the Human Genetics of Neurological Disorders Unit at San Raffaele Scientific Institute. Imputation to reference genome from Haplotype Reference Consortium[2] r1.1 had been conducted on the entire cohort, using Eagle2 for phasing and Minimac4 for missing genotype imputation. Since individuals had been genotyped on four different platforms (Illumina OmniExpress, Illumina Omni 2.5, Illumina Human Quad, Illumina Global Screening Array), imputation was carried out separately on each platform with later merging on bona-fide imputed variants. Given the high level of overlap between OmniExpress and Omni 2.5, samples genotyped on these two platforms were jointly quality-controlled and imputed, retaining only markers with good imputation quality (Rsq>0.6). Variants' rsIDs were assigned from dbSNP v151 GRCh37p13 (http://www.ncbi.nlm.nih.gov/SNP/).

Prior to imputation, a set of homogeneous quality control (QC) metrics at sample and SNP level were conducted for each of the cohorts separately. At sample level, we excluded subjects for which a mismatch with declared sex was observed, those with call-rate < 90% and outliers exceeding the mean level of heterozygosity by >3 standard deviations. At variant level, we discarded rare SNPs with Minor Allele Frequency (MAF) <1%, SNPs with a call-rate<90% and those departing from Hardy-Weinberg Equilibrium (HWE) at $p < 1 \times 10^{-6}$.

From the entire available cohort, patients were screened to match the inclusion criteria for RR-MS and SP-MS and were included in the genetic association study here described. We initially identified 772 patients fulfilling the inclusion criteria, out of which we excluded 13 subjects who had not passed the imputation QC.

Additional study-specific QC was conducted on the remaining 759 subjects and 9,388,047 imputed genetic variants. First, we applied a filter for missingness ≥ 0.02 (no subject was excluded). To discover individuals with potential genetic relationship, we performed pairwise identity by descent (IBD) estimate, identifying 6 potentially related subjects (PI_HAT ≥ 0.250). For each pair, we randomly selected and removed one subject (n=3). To identify population outliers (more than ±6 standard deviations from population mean), we run a Principal Component Analysis (PCA) and excluded one subject. The final number of subjects included in the study was 755. For both IBD estimation and PCA, the regions with extended linkage disequilibrium (LD) were removed and the dataset was pruned (no pair of SNPs with $r^2 > 0.1$ in a window of 1000 kb).

Subsequently, we filtered out all the SNPs with MAF ≤ 0.05, genotyping call rate < 99% and HWE ($P<1x10^{-6}$), for a total of 4,272,520 genetic variants in 755 subjects that were included in the study.

Selection of SNPs in iron metabolism genes

To provide a comprehensive list of genes involved in iron metabolism, we manually screened Gene Ontology and Human Phenotype terms related to iron homeostasis[3]. This list of genes was merged with the Kyoto Encyclopedia of Genes and Genome '*Ferroptosis*' pathway[4]. In total, we identified 336 unique genes relevant to iron metabolism. GRCh37/hg19 genes coordinates were extracted using UCSC Table Browser[5]. In total, 334 out of 336 genes were mapped, and the longest isoform was selected, adding a 2 kilobase (kb) flanking region both upstream and downstream of the gene to account for regulatory variation. Complete lists of the pathways and mapped genes are reported in the eTables 1 and 2. A total of 23,019 high coverage imputed SNPs mapped to the selected iron metabolism genes and underwent association analysis.

Genetic association analysis

We tested the association between the 23,019 genetic variants mapping to iron metabolism genes and the course of MS fitting logistic regression models, adjusted for biological sex and the first eight principal components to account for population stratification. An additive model was used to investigate the effect of genotype on disease course. In the additional experiments, we grouped the subjects who were heterozygous or homozygous for the minor allele of the identified variant and compared them to homozygous subjects for the major allele (i.e., TT versus AT/AA), to prevent

potential issues related to a low number of homozygous subjects. PLINK v1.9 software was used for quality control and the association analysis[6].

Estimation of significance level for genetic association analysis

To calculate a threshold for statistical significance that was able to provide robust results despite multiple testing, we estimated the haplotype blocks in the whole-genome imputed ITA cohort data using PLINK v1.9[6,7]. We identified a total of 828 blocks in the 334 iron metabolism genes. On this number, we applied a Bonferroni correction to minimize the risk of type I error. Following this approach, the threshold for statistical significance was established at $P<6.04x\text{-}10^{-5}$ (0.05/828).

Genotype and quality control in the SWE cohort

Replication of the statistically significant association found in the ITA cohort was conducted in the SWE cohort. Genotyping in the SWE cohort had been performed for previous studies using the Illumina Human OmniExpress platform, carried out by deCODE Genetics (Reykjavik, Iceland). Quality control had been applied as follows. The cohort was initially aligned to the forward strand of the GRC37/hg19 reference genome, according to strand details from the Illumina array manifest files. Any samples presenting with a genotyping yield less than 95% or displaying an inconsistency between stated sex and genetic sex were excluded. This determination was based on a LD pruned set of high-quality chromosome X variants with less than 2% missingness and a MAF higher than 5%. The screening process for variants included conditions such as genotype missingness < 2%, deviation from HWE with $P<1x10^{-6}$ for non-MS individuals, MAF >1%, and a differential missingness between MS and non-MS individuals with $P>1x10^{-4}$. For palindromic variants, alternative allele frequencies were set between 0.4 and 0.6. Individuals demonstrating an absolute inbreeding coefficient > 0.05 or relatedness at the third degree or closer were not included. Before imputation, PCs were calculated, and the samples were projected onto the PC space of 1000 Genomes phase 3 samples. Any samples that deviated more than 6 standard deviations from the mean of the European superpopulation were disregarded. Genotyped data management was performed using PLINK v1.9. During imputation, phasing of 20 Mb blocks, including 5 Mb overlapping flank regions, was conducted using Eagle2 (version v2.4.1), with the number of conditioning haplotypes set to 20,000 (default 10,000). The Haplotype Reference Consortium (HRC; version 1.1) imputation reference panel was employed in the application of Minimac4 for the imputation process. Quality control was conducted by reviewing chromosome continuity, evaluating imputation quality according to chromosome position, and comparing allele frequency with the reference panel. For variants with MAF $\geq$ 0.01, the median imputation quality (R^2) ranged from 0.965 to 0.985, and the median imputation accuracy for genotyped variants (EmpR) spanned from 0.977 to 0.997. Imputed variants with MAF < 0.01 or R2 <0.3 were not included, which resulted in a total of 7,743,331 available autosomal variants.

Replication in the SWE cohort

From whole-genome imputed data, we extracted the subjects and SNPs relevant to our analysis. To replicate significant association found in the ITA cohort, the threshold for statistical significance was set at $p < 0.05$, given that only one signal had passed the threshold for statistical significance after multiple testing correction. As lead variant of the signal in the SWE cohort we considered the SNP having the lowest p-value among those in almost perfect linkage disequilibrium ($r^2 \geq 0.95$) with rs11621525 (eTable 4). The association analysis was conducted using logistic regression, adjusting for biological sex and the first eight principal components, as reported for the ITA cohort.

Effect of genotype on gene expression

Inclusion criteria, genotyping and transcriptomic profiling

For the study on the effect of the rs11621525 variant on *HIF1A* gene expression, inclusion criteria were: a) diagnosis of RR-MS; b) fully naive from disease-modifying treatment (DMT) at the time of sampling; c) no treatment with corticosteroid drugs in the 30 days before sampling; d) availability of rs11621525 genotype.

Genotype information for these patients had been acquired using Illumina OmniExpress beadchips, and imputation had been carried out on a larger cohort available at San Raffaele Scientific Institute, as described above.

For the RNA-sequencing experiment, after blood sampling, Peripheral Blood Mononuclear Cells (PBMC) were isolated through density gradient using Lymphoprep (StemCell Technologies) and RNA was extracted using Quick-DNA/RNA Miniprep Plus (Zymo). The transcriptomic profile was obtained via RNA-seq technology using the Illumina TruSeq Stranded mRNA kit. RNA libraries were sequenced on a HiSeq3000 sequencer (Illumina), reaching >25 million reads/samples.

Bioinformatic pipeline and analysis

RNA-seq reads were aligned to hg19 reference genome, removing poor-quality bases and adapter sequences[8,9]. Quantification of gene expression levels and gene-level summarization was performed using featureCounts[10], according to GENCODE v19 annotation gene model. Quality control of raw and aligned reads was performed by MultiQC tool[11]. To discard features deemed as not expressed, we only retained those with > 5 counts in at least 25% of the whole cohort.

The counts of the *HIF1A* gene were extracted, and the effect of genotype on gene expression was calculated via linear regression applying a dominant model for genotype, using normalized gene counts (z-score) as outcome and genotype as predictor, adjusting for sex and age at sampling.

Effect of genotype on PRL mean volume

MRI acquisition

MRI acquisition was performed separately by the Neuroimaging Research Unit at IRCCS San Raffaele Scientific Institute and by the Department of Neuroradiology at Karolinska University Hospital for patients with available genotype information (see above for detail on genetic data).

For the Italian cohort, a 3.0 Tesla Philips Ingenia CX scanner (Philips Medical Systems) was used. The following sequences were acquired: (a) sagittal three dimensional (3D) fluid attenuation inversion recovery (FLAIR), field of view (FOV)=256×256 mm, voxel size=1×1×1 mm, 192 slices, matrix=256×256, repetition time (TR)=4800 ms, echo time (TE)=270 ms, inversion time (TI)=1650 ms, echo train length (ETL)=167, acquisition time (TA)=6.15 min; (b) sagittal 3D T1-weighted turbo field echo, FOV=256×256, voxel size=1×1×1 mm, 204 slices, matrix=256×256, TR=7 ms, TE=3.2 ms, TI=1000 ms, flip angle=8°, TA=8.53 min; (c) 3D T2-weighted scan, FOV=256×256 mm, pixel size=1×1 mm, 192 axial slices with 1 mm slice thickness, TR 2500 ms, TE 330 ms, ETL=117, TA= 3 min; (c) 3D susceptibility-weighted image (SWI), FOV=230x230, pixel size=0.60×0.60 mm, 135 slices, 2 mm-thick, matrix=384x382, TR=39 ms, TEs=5.5:6:35.5 ms, flip angle=17°, TA=6 min; both magnitude and phase images for each echo were saved.

At the Karolinska University Hospital, brain MRI were acquired using a 3.0 Tesla Siemens MAGNETOM Prisma^{Fit} scanner. The following sequences were acquired: (a) sagittal 3D FLAIR, FOV=256×228 mm, voxel size=1×1×1 mm, 160 slices, matrix=256×228, TR=5000 ms, echo time TE=386 ms, TI=1600 ms, TA=4.52 min; (b) sagittal 3D T1-weighted Magnetization-Prepared Rapid Acquisition Gradient Echo (MPRAGE), FOV=256×256, voxel size=1×1×1 mm, 176 slices, matrix=256×256, TR=1900 ms, TE=2.5 ms, TI=900 ms, flip angle=9°, TA=4.26 min; (c) sagittal 3D T2-weighted (SPACE) turbo spine-echo, FOV=256×256 mm, pixel size=1×1×1 mm, 176 slices, TR 3200 ms, TE 410 ms, TA= 3.49 min; (d) A 3D SWI sequence was acquired with the following protocol: FOV=220x200, pixel size=0.90×0.90 mm, 72 slices, 2 mm-thick, matrix=244x222, TR=28 ms, TEs=20 ms, flip angle=15°, TA=4.37 min; both magnitude and phase images for each echo were saved.

Identification of the PRL and volume extraction

A fully automated approach using the 3D FLAIR and 3D T1weighted as input images[12] was used by Neuroimaging Research Unit at San Raffaele Scientific Institute to identify brain T2-hyperintense WM lesions. T2-hyperintense WM lesion volume was obtained for each patient from their lesion masks, after a careful visual check of the results provided by the automatic segmentation by a team of expert neurologists. The MRI team at the Department of Neuroradiology at Karolinska University Hospital similarly identified brain T2-hyperintense WM lesions using a semi-automated approach, beginning with automatic segmentation using lesion segmentation toolbox lesion prediction algorithm[13] followed by manual edits first by an experienced rater and a trained radiology resident to be finally approved together with a neuroradiologist for consensus agreement.

The PRL were defined as discrete FLAIR-hyperintense lesions either completely or partially surrounded by a paramagnetic rim of hypointense signal in unwrapped phase images.

For each patient, the number and volume of total T2-hyperintense WM lesions as well as of T2-hyperintense WM lesions with or without the hypointense paramagnetic rim were automatically estimated. Firstly, from the global lesion mask, different intensity values were manually given according to the different type of lesions (1=non-paramagnetic rim lesion, 2=paramagnetic rim lesion) creating a new label mask. Then, an automatic pipeline estimated the number and the dimension of the 3D connected objects (lesions) found within label masks, separately for each type of lesion (intensity value). Total number of T2-hyperintense WM lesions was obtained from the sum of T2-hyperintense WM lesions with or without the hypointense paramagnetic rim. Volumes were finally obtained by correcting the dimension for the voxel size and converted in milliliters (ml).

Statistical analysis

Given the non-normal distribution of the volumetric information (Shapiro-test $p<0.001$), the mean volumes of the PRL were rank-based inverse transformed to be suitable for testing using a linear model. The impact of genotype on the lesion mean volume was first assessed independently in the two cohorts through linear regression, adjusting for disease duration, and then meta-analyzed using a fixed-effect model.

Spinal cord pathology

HIF1A genotyping, staining and lesions classification

Cervical, thoracic, and lumbar spinal cord sections from a human autopsy cohort of pathologically confirmed MS cases (n=53) was obtained from the UK Multiple Sclerosis Tissue Bank in compliance with Human Tissue Act guidelines (REC 08/MRE09/31+5).

DNA extracted from freshly frozen cerebellar tissue from MS cases was used for *HIF1A* rs11621525 genotyping using a custom-made TaqMan SNP Genotyping Assay manufactured by ThermoFisher Scientific.

The study was conducted on 108 samples from 36 cases with TT genotype and on 51 samples from 17 cases who carried the rs11621525 A allele. Cases were matched for demographic variables, including sex, age at death, disease duration, *HLA-DRB1*15:01* status, brain weight and post-mortem interval, as shown in eTable 5.
Formalin-fixed paraffin-embedded 6 µm thick adjacent sections were immunostained using primary antibodies for myelin (PLP, BioRad, #MCA839G), microglia-macrophage (CD68, Dako, #M087601-2), and acute axonal injury (BAPP, Invitrogen, #130200). Areas of demyelination were defined as complete loss of myelin in PLP-stained sections. Stage of white matter lesion (active, mixed active/inactive, and inactive) was determined using established criteria[14]. For each section, masks were drawn to delineate lesional and non-lesional white matter areas, and were subsequently superimposed to adjacent sections to allow quantification of the expression of other primary antibodies. In each region of interest, microglia-macrophage inflammation was quantified using a color-based extraction software (chromogen-positive pixels/mm^2), while BAPP-positive axons were quantified using a positive element detection software (number of positive elements/mm^2)[15]. Sections were also impregnated with Palmgren's silver to demonstrate axons, and axonal density were quantified in the non-lesional anterior and lateral cortico-spinal, and in dorsal columns as described elsewhere[16].

Statistical analysis
Statistical analyses were performed using SPSS version 26 (SPSS, Chicago, IL). Differences in population characteristics between genotype groups were tested using Mann-Whitney or Crosstab Chi-square, as appropriate for variable distribution. To correctly analyze multiple observations per each case, generalized estimating equations were built to compare CD68, BAPP, tract areas and axonal counts (set as dependent variable) between TT and AT/AA *HIF1A* genotypes (set as independent variable), accounting for intra-subject variability. CD68 was added as covariate to the model if significantly different between genotypes, given the known correlation with BAPP[17], and cord level was included to correct analyses on tract area and axonal count. Pairwise comparison between estimated means was performed with Wald Chi-square, which is reported with its p-value. Missing values were treated as randomly missing values.

Neurofilament levels
Plasma NFL
Plasma samples for the study on NFL had been collected and frozen at the Karolinska Institutet and belonged to the IMSE cohort, collected to perform post-marketing disease-modifying treatments monitoring[18]. Plasma NFL levels were determined using a sensitive immunoassay on the Simoa platform through a commercially available NF-Light kit and antibodies from UmanDiagnostics according to the manufacturer's instructions (Quanterix, Lexington, MA), as previously described[19]. Patients were naive or had been treated with glatiramer acetate or interferon and were sampled before the beginning of the first or a new DMT. To study the effect of *HIF1A* genotype on plasma NFL levels, starting from this dataset we extracted all the patients belonging to the SWE cohort used for the genetic analysis and that had been sampled before 20 years from disease onset, when they had still a RR-MS course and were not in a relapse.
When evaluating the response to a new DMT in terms of change in plasma NFL, starting from the original IMSE cohort described above, we included all the RR-MS patients within 20 years from onset that had been sampled longitudinally at baseline and after treatment start (12±6 months).

CSF NFL
CSF NFL samples had been collected at the Karolinska Institutet at the time of neurological assessment that led to the diagnosis of MS[20]. NFL levels in the CSF were measured using commercially available ELISA kits (Uman diagnostics, Umeå, Sweden) according to the manufacturers' instructions.

NFL levels analysis
All NFL levels were used in linear models in the form of a z-score, after rank-based inverse normal transformation[21]. Plasma NFL levels were adjusted for body mass index and age at sampling as suggested by recent literature[22]; moreover, disease duration at sampling and line of treatment (first versus second line) about to start were used as covariates. In the CSF analysis, the NFL levels were adjusted for disease duration and age at sampling. To assess the effect of treatment on NFL reduction over time, we used mixed-effects linear models, to account for intra-subject variation and adjusting for disease duration.

Pharmacogenomic study of dimethyl fumarate
We evaluated how the rs11621525 genotype affected the response to dimethyl fumarate (DMF), using the No Evidence of Disease Activity status[23] (NEDA-3) at two years from treatment start as outcome of disease activity. The NEDA-3 status was defined when all of the following criteria were satisfied over the 2-years follow-up: a) no new relapses; b) no new/enlarging or gadolinium enhancing lesions at brain MRI; c) no Expanded Disability Status Scale (EDSS) progression over the follow-up. EDSS progression was defined as follows: a) an increase of at least 1.5 points for patients with baseline EDSS = 0; b) an increase of at least 1.0 point for baseline EDSS between 1.0 and 5.5; c) increase of at least 0.5 point for baseline EDSS ≥ 6.0.
From the cohort of patients with available whole-genome imputed genetic data, that are part of the cohort available at the Laboratory of Human Genetics of Neurological Disorders at San Raffaele Scientific Institute described above, we

identified 138 patients that fulfilled the following inclusion criteria: 1) diagnosis of RR-MS; 2) patients not previously treated with second line DMT or other immunosuppressive drugs; 3) continuous DMF treatment for at least 2-years or shift to other DMT for lack of efficacy of DMF; 4) availability of clinical information to define the NEDA-3 status at two-years from DMF start. Patients who discontinued DMF treatment for side effects within the first 2 years, with no evidence of disease activity under treatment, were not included in the analysis given that the NEDA-3 status could not be assessed at 2-year follow-up. Logistic regression was used to assess the effect of rs11621525 genotype (as predictor) on the NEDA-3 status at 2-years from treatment start (as outcome), adjusting for age at disease onset and sex.

Ethics committees approval

Patients participating to this study had given written informed consent and the studies had been approved locally by the respective ethical committee. Local approval numbers are as follows. San Raffaele Scientific Institute: 1013/DG, 274/DG, 397/ER/mm, 851/DG, 20/int/2019. Karolinska Institutet: 02-548, 2006/845-31/1, 2009/2107-31/2. 2011/641-31/4, 02-548, 2015/2235-32/4, 2015/2236-32, 2015/2260-32/2, 2016/1167-32, 2016/1168-32, 2016/1169-32, 2017/1347-32, 2017/1348-32, 2017/1349-32, 2017/1350-32, 2017/1426-32. Oxford Neuroinflammation Center: REC-08/MRE09/31+5.

SUPPLEMENTARY FIGURES

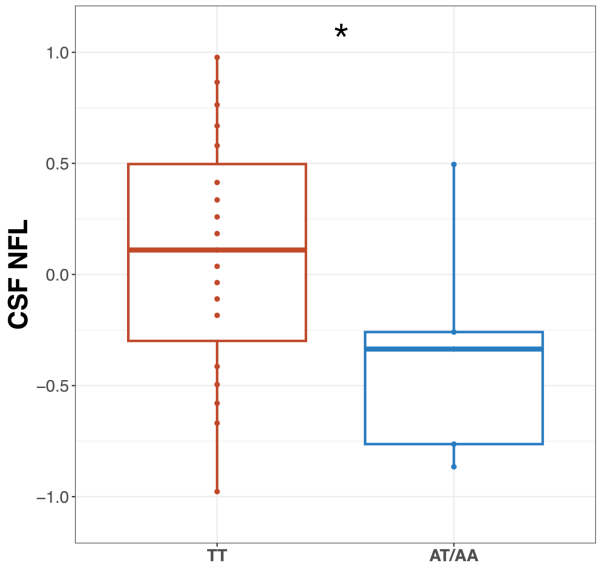

eFigure 1. CSF NFL levels in CIS.
On the x-axis the genotype for rs1951795 variant (tagging rs11621525) is shown; on the y-axis the z-score for normalized CSF NFL levels is reported. * = P < .05. CIS: Clinically Isolated Syndrome

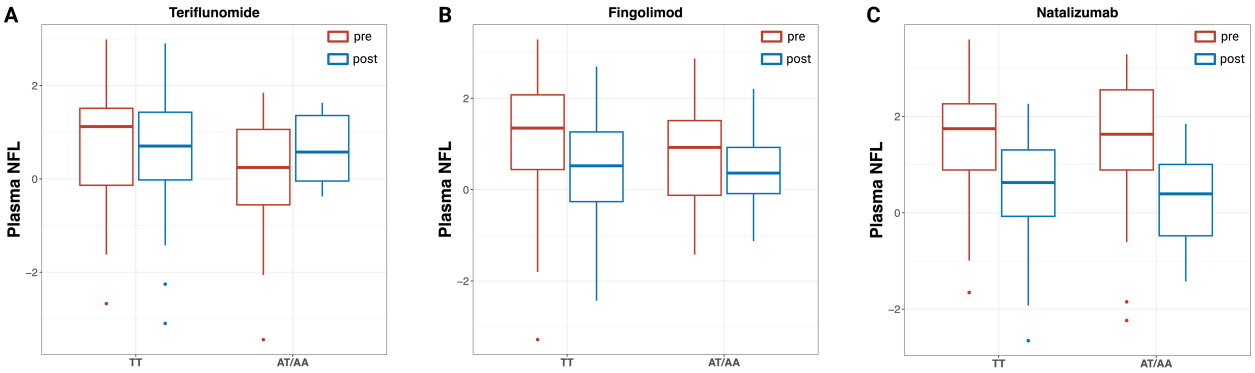

eFigure 2. Effect of HIF1A genotype on plasma NFL levels change after the start of treatment with teriflunomide, fingolimod and natalizumab.

On the x-axis the genotype for rs1951795 variant (tagging rs11621525) is shown; on the y-axis the z-score for normalized plasma NFL levels before (in red; "pre") and after (in blue; "post") treatment start for teriflunomide (panel A), fingolimod (panel B) and natalizumab (panel C). The reduction of plasma NFL levels after treatment start is clearly visible for Fingolimod and Natalizumab, and only in the TT group for Teriflunomide; no significant additional effect of the *HIF1A* rs1951795 SNP on the NFL levels emerged, despite what observed in the DMF group (see main manuscript, Figure 4C).

SUPPLEMENTARY TABLES

eTable 1. List of the selected iron metabolism gene sets.

In the leftmost column the name of the gene set is reported, as coded in the respective source (GO = Gene Ontology; HP = Human Phenotype; KEGG = Kyoto Encyclopedia of Genes and Genomes). N of genes = number of genes in the gene set.

Gene set	*Source*	*N of genes*
GOBP_IRON_ION_TRANSPORT	GO	79
GOBP_CELLULAR_IRON_ION_HOMEOSTASIS	GO	70
GOBP_RESPONSE_TO_IRON_ION	GO	28
GOBP_RESPONSE_TO_IRON_II_ION	GO	5
GOBP_RESPONSE_TO_IRON_III_ION	GO	5
GOBP_IRON_SULFUR_CLUSTER_ASSEMBLY	GO	24
GOBP_IRON_IMPORT_INTO_CELL	GO	11
GOBP_IRON_ION_TRANSMEMBRANE_TRANSPORT	GO	19
GOBP_REGULATION_OF_IRON_ION_TRANSPORT	GO	9
GOBP_REGULATION_OF_IRON_ION_TRANSMEMBRANE_TRANSPORT	GO	6
GOBP_IRON_ION_HOMEOSTASIS	GO	86
GOBP_MULTICELLULAR_ORGANISMAL_IRON_ION_HOMEOSTASIS	GO	7
GOBP_CELLULAR_RESPONSE_TO_IRON_ION	GO	9
GOBP_PROTEIN_MATURATION_BY_IRON_SULFUR_CLUSTER_TRANSFER	GO	16
GOBP_SEQUESTERING_OF_IRON_ION	GO	7
GOBP_IRON_ION_IMPORT_ACROSS_PLASMA_MEMBRANE	GO	6
GOBP_IRON_COORDINATION_ENTITY_TRANSPORT	GO	14
GOMF_IRON_ION_TRANSMEMBRANE_TRANSPORTER_ACTIVITY	GO	10
GOMF_IRON_ION_BINDING	GO	150
GOMF_FERROUS_IRON_BINDING	GO	26
GOMF_FERRIC_IRON_BINDING	GO	10
HP_ABNORMALITY_OF_IRON_HOMEOSTASIS	HP	19
HP_IRON_ACCUMULATION_IN_BRAIN	HP	9
KEGG_FERROPTOSIS	KEGG	41

eTable 2. List of the mapped genes in iron metabolism included in the genetic analysis.
For each of the 334 included genes, chromosome (CHR), positional information of the gene in base-pairs according to GRCh37/hg19 reference genome (START, END) and gene symbol (GENE) according to HUGO Gene Nomenclature Committee are reported. The final region included in the analysis (START-2kb and END+2kb) is also shown, representing the gene body with a 2 kilobase (kb) window at end. See full text for details.

CHR	*START*	*END*	*GENE*	*START-2kb*	*END+2kb*
1	11994723	12035599	PLOD1	11992723	12037599
1	17312452	17338423	ATP13A2	17310452	17340423
1	22963117	22966175	C1QA	22961117	22968175
1	43212005	43232755	P3H1	43210005	43234755
1	44440601	44443972	ATP6V0B	44438601	44445972
1	44462154	44483012	SLC6A9	44460154	44485012
1	47264669	47285021	CYP4B1	47262669	47287021
1	47308766	47366147	CYP4Z2P	47306766	47368147
1	47394845	47407156	CYP4A11	47392845	47409156
1	47489239	47516423	CYP4X1	47487239	47518423
1	47533159	47583992	CYP4Z1	47531159	47585992
1	47603106	47614526	CYP4A22	47601106	47616526
1	60358979	60392423	CYP2J2	60356979	60394423
1	94352589	94375012	GCLM	94350589	94377012
1	109648572	109656479	C1orf194	109646572	109658479
1	145413190	145417545	HJV	145411190	145419545
1	155259083	155271225	PKLR	155257083	155273225
1	198492351	198510075	ATP6V1G3	198490351	198512075
1	213031596	213072705	FLVCR1	213029596	213074705
1	220087605	220101993	SLC30A10	220085605	220103993
1	228353428	228369958	IBA57	228351428	228371958
1	231499496	231560790	EGLN1	231497496	231562790
1	235530727	235612280	TBCE	235528727	235614280
1	242158791	242162385	MAP1LC3C	242156791	242164385
2	3501689	3523350	ADI1	3499689	3525350
2	10861774	10925236	ATP6V1C2	10859774	10927236
2	31557187	31637611	XDH	31555187	31639611
2	38294745	38303323	CYP1B1	38292745	38305323
2	42994228	43019751	HAAO	42992228	43021751
2	46524540	46613842	EPAS1	46522540	46615842
2	46755024	46769141	ATP6V1E2	46753024	46771141
2	47168312	47303275	TTC7A	47166312	47305275
2	69623244	69664760	NFU1	69621244	69666760
2	70314584	70316334	PCBP1	70312584	70318334
2	71162997	71192561	ATP6V1B1	71160997	71194561
2	72356366	72374991	CYP26B1	72354366	72376991
2	86668583	86719839	KDM3A	86666583	86721839
2	96931883	96939900	CIAO1	96929883	96941900
2	119981383	120023227	STEAP3	119979383	120025227
2	127941411	127963343	CYP27C1	127939411	127965343
2	131095815	131099922	CCDC115	131093815	131101922
2	172378865	172414643	CYBRD1	172376865	172416643
2	190425315	190445537	SLC40A1	190423315	190447537
2	200793633	200820459	TYW5	200791633	200822459
2	201450730	201536217	AOX1	201448730	201538217
2	204103163	204170563	CYP20A1	204101163	204172563
2	219246751	219261617	SLC11A1	219244751	219263617
2	219524378	219528166	BCS1L	219522378	219530166
2	219646471	219680016	CYP27A1	219644471	219682016
2	220074487	220085174	RP11-803J6.1, ABCB6	220072487	220087174
2	223725731	223808119	ACSL3	223723731	223810119
2	239072632	239077515	ERFE	239070632	239079515
3	3168599	3190706	TRNT1	3166599	3192706
3	11314009	11599139	ATG7	11312009	11601139

3	42913683	42917633	CYP8B1	42911683	42919633
3	46477495	46506598	LTF	46475495	46508598
3	48601505	48632593	COL7A1	48599505	48634593
3	49027340	49044581	P4HTM	49025340	49046581
3	50355220	50360281	HYAL2	50353220	50362281
3	71003864	71180092	FOXP1	71001864	71182092
3	113465865	113530905	ATP6V1A	113463865	113532905
3	133464799	133497850	TF	133462799	133499850
3	145787227	145879282	PLOD2	145785227	145881282
3	148890289	148939832	CP	148888289	148941832
3	184428154	184429836	MAGEF1	184426154	184431836
3	186383797	186396023	HRG	186381797	186398023
3	189674516	189838908	P3H2	189672516	189840908
3	195776154	195809032	TFRC	195774154	195811032
3	196728611	196756687	MELTF	196726611	196758687
4	15606006	15657035	FBXL5	15604006	15659035
4	76781025	76823681	PPEF2	76779025	76825681
4	83550689	83720010	SCD5	83548689	83722010
4	89011415	89080011	ABCG2	89009415	89082011
4	90645249	90759447	SNCA	90643249	90761447
4	103182820	103266655	SLC39A8	103180820	103268655
4	103998781	104021024	BDH2	103996781	104023024
4	106067841	106200960	TET2	106065841	106202960
4	108852716	108874613	CYP2U1	108850716	108876613
4	129190391	129209984	PGRMC2	129188391	129211984
4	139085247	139163503	SLC7A11	139083247	139165503
4	146019155	146050676	ABCE1	146017155	146052676
4	166248817	166264314	MSMO1	166246817	166266314
4	185676748	185747215	ACSL1	185674748	185749215
4	187112673	187134617	CYP4V2	187110673	187136617
5	1392904	1445543	SLC6A3	1390904	1447543
5	68462836	68474070	CCNB1	68460836	68476070
5	94799598	94890709	TTC37	94797598	94892709
5	115140429	115152405	CDO1	115138429	115154405
5	121187649	121188523	FTMT	121185649	121190523
5	131285666	131347355	ACSL6	131283666	131349355
5	131584600	131631008	P4HA2	131582600	131633008
5	133492081	133512724	SKP1	133490081	133514724
5	137890570	137911318	HSPA9	137888570	137913318
5	141488323	141534008	NDFIP1	141486323	141536008
5	154198051	154230213	FAXDC2	154196051	154232213
5	172410762	172461900	ATP6V0E1	172408762	172463900
6	5186833	5261172	LYRM4	5184833	5263172
6	7727010	7881961	BMP6	7725010	7883961
6	10396915	10415470	TFAP2A	10394915	10417470
6	26087508	26095469	HFE	26085508	26097469
6	31512227	31514625	ATP6V1G2	31510227	31516625
6	31926580	31937532	SKIV2L	31924580	31939532
6	31973358	31976712	CYP21A1P, CYP21A	31971358	31978712
6	32006092	32009447	CYP21A2	32004092	32011447
6	38136226	38607924	BTBD9	38134226	38609924
6	46517444	46620523	CYP39A1	46515444	46622523
6	53362139	53409927	GCLC	53360139	53411927
6	106632351	106773695	ATG5	106630351	106775695
7	1022834	1029276	CYP2W1	1020834	1031276
7	6061877	6098860	EIF2AK1	6059877	6100860
7	15239942	15601640	AGMO	15237942	15603640
7	39606002	39612480	YAE1	39604002	39614480
7	87834431	87849399	SRI	87832431	87851399
7	87905743	87936228	STEAP4	87903743	87938228
7	89783688	89794141	STEAP1	89781688	89796141

7	89840999	89866992	STEAP2	89838999	89868992
7	91741462	91763840	CYP51A1	91739462	91765840
7	97736196	97838944	LMTK2	97734196	97840944
7	99282301	99332819	CYP3A7-CYP3A51P, CYP3A7	99280301	99334819
7	99354582	99381811	CYP3A4	99352582	99383811
7	99425635	99464173	CYP3A43	99423635	99466173
7	100218038	100239201	TFR2	100216038	100241201
7	100849257	100861011	PLOD3	100847257	100863011
7	128502856	128505903	ATP6V1F	128500856	128507903
7	138391038	138458782	ATP6V0A4	138389038	138460782
7	139528951	139720125	TBXAS1	139526951	139722125
7	139784545	139876741	KDM7A	139782545	139878741
7	148395932	148498202	CUL1	148393932	148500202
7	149570056	149577787	ATP6V0E2	149568056	149579787
7	150745378	150749843	ASIC3	150743378	150751843
8	20054703	20079207	ATP6V1B2	20052703	20081207
8	22225049	22280249	SLC39A14	22223049	22282249
8	23386362	23430063	SLC25A37	23384362	23432063
8	27727398	27850369	SCARA5	27725398	27852369
8	42249278	42263455	VDAC3	42247278	42265455
8	54628102	54755871	ATP6V1H	54626102	54757871
8	59402736	59412720	CYP7A1	59400736	59414720
8	65508528	65711348	CYP7B1	65506528	65713348
8	87111138	87166454	ATP6V0D2	87109138	87168454
8	104033247	104085285	ATP6V1C1	104031247	104087285
8	128748314	128753680	MYC	128746314	128755680
8	143953772	143961236	CYP11B1	143951772	143963236
8	143991974	143999259	CYP11B2	143989974	144001259
9	32384600	32450832	ACO1	32382600	32452832
9	71650478	71693993	FXN	71648478	71695993
9	79792360	80032399	VPS13A	79790360	80034399
9	88879462	88897490	ISCA1	88877462	88899490
9	96338908	96441869	PHF2	96336908	96443869
9	116148591	116163618	ALAD	116146591	116165618
9	117349993	117361152	ATP6V1G1	117347993	117363152
9	130911731	130915734	LCN2	130909731	130917734
9	139257440	139268133	CARD9	139255440	139270133
9	140100118	140113813	NDOR1	140098118	140115813
10	13319795	13342130	PHYH	13317795	13344130
10	45869623	45941567	ALOX5	45867623	45943567
10	48413091	48416853	GDF2	48411091	48418853
10	51565107	51590734	NCOA4	51563107	51592734
10	70320116	70454239	TET1	70318116	70456239
10	74766979	74856732	P4HA1	74764979	74858732
10	76969911	76991207	VDAC2	76967911	76993207
10	90965693	90967071	CH25H	90963693	90969071
10	94821020	94828454	CYP26C1	94819020	94830454
10	94833646	94837641	CYP26A1	94831646	94839641
10	96522462	96612671	CYP2C19	96520462	96614671
10	96698414	96749148	CYP2C9	96696414	96751148
10	96796528	96829254	CYP2C8	96794528	96831254
10	99218080	99258366	MMS19	99216080	99260366
10	101370274	101380221	SLC25A28	101368274	101382221
10	102106771	102124588	SCD	102104771	102126588
10	102295640	102313681	HIF1AN	102293640	102315681
10	104590287	104597290	CYP17A1	104588287	104599290
10	114135955	114188138	ACSL5	114133955	114190138
10	131934638	131977932	GLRX3	131932638	131979932
10	135340866	135352620	CYP2E1	135338866	135354620
11	568088	568198	MIR210	566088	570198

11	2185158	2193035	TH	2183158	2195035
11	5246695	5248301	HBB	5244695	5250301
11	6452267	6462254	HPX	6450267	6464254
11	14899555	14913751	CYP2R1	14897555	14915751
11	18042083	18062335	TPH1	18040083	18064335
11	27062508	27149354	BBOX1	27060508	27151354
11	31391376	31454382	DNAJC24	31389376	31456382
11	34937676	35017675	PDHXPDX1	34935676	35019675
11	43902356	43941825	ALKBH3	43900356	43943825
11	46698624	46722215	ARHGAP1	46696624	46724215
11	61731756	61735132	FTH1	61729756	61737132
11	62623483	62656355	SLC3A2	62621483	62658355
11	67806461	67818366	TCIRG1	67804461	67820366
11	69455872	69469242	CCND1	69453872	69471242
11	69480331	69490165	LTO1	69478331	69492165
11	73977701	74022699	P4HA3	73975701	74024699
11	85668213	85780139	PICALM	85666213	85782139
11	93754377	93847374	HEPHL1	93752377	93849374
11	107373452	107436461	ALKBH8	107371452	107438461
11	110300660	110335608	FDX1	110298660	110337608
11	111895537	111935002	DLAT	111893537	111937002
11	113280316	113346001	DRD2	113278316	113348001
11	119531702	119599435	NECTIN1	119529702	119601435
11	121163387	121184119	SC5D	121161387	121186119
12	7085346	7125842	LPCAT3	7083346	7127842
12	27849427	27850566	REP15	27847427	27852566
12	46576840	46663208	SLC38A1, SAT1	46574840	46665208
12	46751970	46766645	SLC38A2, SAT2	46749970	46768645
12	48166966	48176536	SLC48A1	48164966	48178536
12	51379774	51422058	SLC11A2	51377774	51424058
12	53845885	53874946	PCBP2	53843885	53876946
12	58156116	58160976	CYP27B1	58154116	58162976
12	67663060	67708388	CAND1	67661060	67710388
12	68548549	68553521	IFNG	68546549	68555521
12	72332625	72426221	TPH2	72330625	72428221
12	103232103	103311381	PAH	103230103	103313381
12	108956293	108963160	ISCU	108954293	108965160
12	109525992	109531293	ALKBH2	109523992	109533293
12	116997185	117014425	MAP1LC3B2	116995185	117016425
12	123459353	123464588	OGFOD2	123457353	123466588
12	124196864	124246301	ATP6V0A2	124194864	124248301
13	28494167	28500451	PDX1	28492167	28502451
14	23815526	23821660	SLC22A17	23813526	23823660
14	32030590	32330429	NUBPL	32028590	32332429
14	34393420	34420284	EGLN3	34391420	34422284
14	62162118	62214977	HIF1A	62160118	62216977
14	67804580	67826720	ATP6V1D	67802580	67828720
14	74960422	74962271	ISCA2	74958422	74964271
14	76044939	76114512	FLVCR2	76042939	76116512
14	78138748	78174356	ALKBH1	78136748	78176356
14	96001322	96011055	GLRX5	95999322	96013055
14	100150754	100193638	CYP46A1	100148754	100195638
15	43489425	43513323	EPB42	43487425	43515323
15	45003684	45010357	B2M	45001684	45012357
15	51500253	51630795	CYP19A1	51498253	51632795
15	64364760	64386207	CIAO2A	64362760	64388207
15	69307033	69349501	NOX5	69305033	69351501
15	69706626	69740764	KIF23	69704626	69742764
15	73344824	73597547	NEO1	73342824	73599547
15	74630102	74660081	CYP11A1	74628102	74662081
15	75011882	75017877	CYP1A1	75009882	75019877

15	75041183	75048941	CYP1A2	75039183	75050941
15	78730517	78793798	IREB2	78728517	78795798
16	202853	204504	HBZ	200853	206504
16	222845	223709	HBA2	220845	225709
16	226678	227520	HBA1	224678	229520
16	230332	231178	HBQ1	228332	233178
16	779768	790997	CIAO3	777768	792997
16	1832932	1839192	NUBP2	1830932	1841192
16	2563726	2570224	ATP6V0C	2561726	2572224
16	4526340	4560348	HMOX2	4524340	4562348
16	10837697	10863208	NUBP1	10835697	10865208
16	29464913	29466285	BOLA2	29462913	29468285
16	30204255	30205627	BOLA2B	30202255	30207627
16	53737874	54148379	FTO	53735874	54150379
16	56485423	56511407	OGFOD1	56483423	56513407
16	57462086	57481369	CIAPIN1	57460086	57483369
16	66965957	66968326	CIAO2B	66963957	66970326
16	67471916	67515089	ATP6V0D1	67469916	67517089
16	74746855	74808729	FA2H	74744855	74810729
16	87425800	87438380	MAP1LC3B	87423800	87440380
17	4534213	4544971	ALOX15	4532213	4546971
17	6899383	6914055	ALOX12	6897383	6916055
17	7529555	7531194	SAT2	7527555	7533194
17	7571719	7590868	TP53	7569719	7592868
17	7942357	7952451	ALOX15B	7940357	7954451
17	7975953	7991021	ALOX12B	7973953	7993021
17	7999217	8022234	ALOXE3	7997217	8024234
17	26684686	26689089	TMEM199	26682686	26691089
17	26721660	26733230	SLC46A1	26719660	26735230
17	36886509	36891858	CISD3	36884509	36893858
17	40610861	40674597	ATP6V0A1	40608861	40676597
17	40962149	40976310	BECN1	40960149	40978310
17	57697049	57774317	CLTC	57695049	57776317
17	74523429	74533987	CYGB	74521429	74535987
17	74708913	74722881	JMJD6	74706913	74724881
17	80347085	80376513	OGFOD3	80345085	80378513
18	48556582	48611411	SMAD4	48554582	48613411
18	55212072	55253969	FECH	55210072	55255969
18	60790578	60986613	BCL2	60788578	60988613
19	1104648	1106787	GPX4	1102648	1108787
19	3490818	3500621	DOHH	3488818	3502621
19	7587495	7598895	MCOLN1	7585495	7600895
19	8455204	8469317	RAB11B	8453204	8471317
19	10828728	10942586	DNM2	10826728	10944586
19	11685474	11689801	ACP5	11683474	11691801
19	13049413	13055304	CALR	13047413	13057304
19	15619335	15663128	CYP4F22	15617335	15665128
19	15726028	15740447	CYP4F8	15724028	15742447
19	15751706	15771570	CYP4F3	15749706	15773570
19	15783827	15807984	CYP4F12	15781827	15809984
19	15988833	16008884	CYP4F2	15986833	16010884
19	16023179	16045676	CYP4F11	16021179	16047676
19	35773409	35776045	HAMP	35771409	35778045
19	41305333	41314346	EGLN2	41303333	41316346
19	41349442	41356352	CYP2A6	41347442	41358352
19	41381343	41388657	CYP2A7	41379343	41390657
19	41396730	41406413	CYP2A6	41394730	41408413
19	41497203	41524301	CYP2B6	41495203	41526301
19	41594355	41602100	CYP2A13	41592355	41604100
19	41620352	41634281	CYP2F1	41618352	41636281
19	41699114	41713444	CYP2S1	41697114	41715444

19	44010870	44031396	ETHE1	44008870	44033396
19	49468565	49470136	FTL	49466565	49472136
19	54926604	54947899	TTYH1	54924604	54949899
20	3869741	3904502	PANK2	3867741	3906502
20	4666796	4682234	PRNP	4664796	4684234
20	6748744	6760910	BMP2	6746744	6762910
20	33146500	33148149	MAP1LC3A	33144500	33150149
20	33516235	33543601	GSS	33514235	33545601
20	34256609	34287287	NFS1	34254609	34289287
20	48120410	48184707	PTGIS	48118410	48186707
20	52769987	52790516	CYP24A1	52767987	52792516
21	33031934	33041243	SOD1	33029934	33043243
21	43782390	43786644	TFF1	43780390	43788644
22	18074902	18111588	ATP6V1E1	18072902	18113588
22	29138042	29153496	HSCB	29136042	29155496
22	35777059	35790207	HMOX1	35775059	35792207
22	37461478	37499693	TMPRSS6	37459478	37501693
22	38507501	38577761	PLA2G6	38505501	38579761
22	41865128	41924993	ACO2	41863128	41926993
22	42522500	42526883	CYP2D6	42520500	42528883
22	42536213	42540575	CYP2D7	42534213	42542575
22	50925212	50928750	MIOX	50923212	50930750
X	18709044	18846034	PPEF1	18707044	18848034
X	23801274	23804327	SAT1	23799274	23806327
X	31089357	31090170	FTHL17	31087357	31092170
X	37639269	37672714	CYBB	37637269	37674714
X	48932091	48937564	WDR45	48930091	48939564
X	53963112	54071569	PHF8	53961112	54073569
X	55035487	55057497	ALAS2	55033487	55059497
X	65382432	65487230	HEPH	65380432	65489230
X	74273006	74376175	ABCB7	74271006	74378175
X	77166193	77305892	ATP7A	77164193	77307892
X	108884563	108976621	ACSL4	108882563	108978621
X	135044230	135056134	MMGT1	135042230	135058134
X	153656977	153664862	ATP6AP1	153654977	153666862
X	153759605	153775233	G6PD	153757605	153777233
X	154718672	154842622	TMLHE	154716672	154844622

eTable 3. Results of the genetic association study in the ITA cohort.

CHR	*SNP*	*POS*	*A1*	*OR SP*	*95% CI*	*P-value*
14	rs11621525	62203056	A	0.57	0.44-0.72	3.30×10^{-6}
14	rs10873142	62203462	C	0.59	0.47-0.75	1.34×10^{-5}
14	rs4899057	62202942	G	0.59	0.47-0.75	1.34×10^{-5}
14	rs4902082	62212675	C	0.59	0.47-0.75	1.34×10^{-5}
14	rs12435848	62176891	A	0.61	0.49-0.77	2.11×10^{-5}
14	rs1951795	62171426	A	0.60	0.48-0.76	2.66×10^{-5}
14	rs12232182	62176220	C	0.65	0.53-0.82	1.50×10^{-4}
14	rs2301111	62200201	G	0.65	0.52-0.81	1.73×10^{-4}
14	rs7153817	62201500	G	0.65	0.52-0.81	1.73×10^{-4}

CHR = chromosome; SNP = Single Nucleotide Polymorphism rsID; POS = position on chromosome (reference genome GRCh37/hg19); A1 = effect allele; OR SP= odds ratio of conversion to SP-MS for A1; 95% CI = 95% Confidence Interval for OR SP; P-value = nominal p-value from logistic regression as described in the Methods.

eTable 4. Replication in the Swedish (SWE) cohort.

CHR	*SNP*	*BP*	*A1*	*NMISS*	*OR SP*	*95% CI*	*P*	*LD*
14	rs11621525	62203056	A	2056	0.80	0.67-0.95	.012	1.00
14	rs10873142	62203462	C	2042	0.79	0.67-0.94	.0080	0.98
14	rs4899057	62202942	G	2045	0.80	0.67-0.94	.0087	0.98
14	rs4902082	62212675	C	2032	0.80	0.67-0.95	.0095	0.98
14	rs1951795	62171426	A	2062	0.79	0.67-0.94	.0079	0.98

CHR = chromosome; SNP = Single Nucleotide Polymorphism rsID; POS = position on chromosome (reference genome GRCh37/hg19); A1 = effect allele; NMISS = number of observations (=final number of subjects with non-missing genotype, phenotype or covariates); OR SP= odds ratio of conversion to SP-MS course for A1; 95% CI = 95% Confidence Interval for OR SP; P-value = nominal p-value from logistic regression; LD = r^2 indicating linkage disequilibrium (LD) with rs11621525.

eTable 5. Characteristics of the cohort included in the post-mortem pathology study.

	TT ***108 samples from 36 cases***	***AT/AA*** ***51 samples from 17 cases***	***p-value***
Sex	F: 64% (23) M: 36% (13)	F: 82% (14) M: 18% (3)	n.s.
Course	SP-MS: 84% (27) PP-MS: 16% (5)	SP-MS: 93% (13) PP-MS: 7% (1)	n.s.
HLA-DRB1*15:01+	53.3% (16)	47% (8)	n.s.
Brain weight (g)	1174 (894-1380)	1132 (931-1300)	n.s.
Post-mortem interval (h)	16.69 (6-28)	20.56 (7-38)	n.s.
Age at death (years)	61.22 (40-92)	65.24 (55-82)	n.s.
Disease duration (years)	29.36 (12-56)	31.19 (17-58)	n.s.

For sex, course and HLA-DRB1*15:01 status, the number of patients (in brackets) and percentages are reported. For brain weight, post-mortem interval, age at death and disease duration mean value and range (in brackets) are reported. The p-value from chi-square test is reported for sex, course, and *HLA-DRB1*15:01* status. For the remaining, p-values from non-parametric Mann-Whitney test are reported. Number of subjects with missing information are as follows (TT group, AT/AA group). Course: 4, 3; *HLA-DRB1*15:01* status: 6, 0; brain weight: 1, 0; disease duration: 0, 1. Abbreviations: M = male; F = female; SP-MS = secondary progressive MS; PP-MS = primary progressive MS; *HLA-DRB1*15:01*+ = positivity for *HLA-DRB1*15:01* allele; g = grams; h = hours; n.s. = not statistically significant.

eTable 6. Effect of *HIF1A* genotype on non-lesional pathology.

	TT, 88 samples from 36 cases		*AT/AA, 40 samples from 17 cases*	
	Mean	**95% Wald CI**	**Mean**	**95% Wald CI**
ACST area (mm^2)	1.58	1.4 to 1.77	1.85	1.42 to 2.28
LCST area (mm2)	3.81	3.34 to 4.28	4.07	3.21 to 4.94
DC area (mm^2)	5.28	4.72 to 5.83	6.33	4.97 to 7.69
ACST total axons	29165	24264 to 34066	39437	28433 to 50442
LCST total axons	59600	47187 to 72013	62523	39918 to 85128
DC total axons	104098	90797 to 117398	128882	86711 to 171054

The table shows the notional tract cross-sectional areas (in mm^2) and total axonal counts in non-lesional anterior cortico-spinal tract (ACST), lateral cortico-spinal tract (LCST), and dorsal columns (DC) in *HIF1A*-TT and -AT/AA subgroups. Estimated mean values and 95% Wald confidence interval (CI) corrected for cord level are displayed; p-values of pairwise comparison between genotype subgroups are ≥ 0.1 and are not reported in the Table.

eTable 7. Impact of *HIF1A* genotype on NFL levels after treatment start.

	N	*Years [SD]*	*Beta*	*95% CI*	*P*
Dimethyl Fumarate	151	1.07 [0.12]	-0.38	-0.71 to -0.043	**.027**
Teriflunomide	52	0.90 [0.24]	-0.40	-0.94 to 0.14	.15
Natalizumab	178	1.06 [0.28]	-0.16	-0.45 to 0.13	.28
Fingolimod	130	1.05 [0.17]	-0.18	-0.57 to 0.21	.36

The table shows the results of the mixed-effects linear models assessing the effect of rs1951795 genotype on the change in plasma NFL levels after treatment start. For each drug, the table reports: the number of subjects included (N), the mean time in years (with SD = standard deviation) between the first plasma NFL measurement (obtained immediately before drug start) and the second plasma NFL measurement (obtained after 12 months with a ±6-month window), the regression coefficient from mixed-effect linear model (beta) and it's 95% confidence interval (CI) and p-values (P) from mixed-effects linear models.

REFERENCES

1. Thompson AJ, Banwell BL, Barkhof F, et al. Diagnosis of multiple sclerosis: 2017 revisions of the McDonald criteria. *Lancet Neurol* 2018;17(2):162–73.
2. the Haplotype Reference Consortium. A reference panel of 64,976 haplotypes for genotype imputation. *Nat Genet* 2016;48(10):1279–83.
3. Ashburner M, Ball CA, Blake JA, et al. Gene Ontology: tool for the unification of biology. *Nat Genet* 2000;25(1):25–9.
4. Kanehisa M. KEGG: Kyoto Encyclopedia of Genes and Genomes. *Nucleic Acids Res* 2000;28(1):27–30.
5. Karolchik D. The UCSC Table Browser data retrieval tool. *Nucleic Acids Res* 2004;32(90001):493D – 496.
6. Chang CC, Chow CC, Tellier LC, Vattikuti S, Purcell SM, Lee JJ. Second-generation PLINK: rising to the challenge of larger and richer datasets. *GigaScience* 2015;4(1):7.
7. Gabriel SB, Schaffner SF, Nguyen H, et al. The Structure of Haplotype Blocks in the Human Genome. *Science* 2002;296(5576):2225–9.
8. Dobin A, Davis CA, Schlesinger F, et al. STAR: ultrafast universal RNA-seq aligner. *Bioinformatics* 2013;29(1):15–21.
9. Bolger AM, Lohse M, Usadel B. Trimmomatic: a flexible trimmer for Illumina sequence data. *Bioinformatics* 2014;30(15):2114–20.
10. Liao Y, Smyth GK, Shi W. featureCounts: an efficient general purpose program for assigning sequence reads to genomic features. *Bioinformatics* 2014;30(7):923–30.
11. Ewels P, Magnusson M, Lundin S, Käller M. MultiQC: summarize analysis results for multiple tools and samples in a single report. *Bioinformatics* 2016;32(19):3047–8.
12. Valverde S, Cabezas M, Roura E, et al. Improving automated multiple sclerosis lesion segmentation with a cascaded 3D convolutional neural network approach. *NeuroImage* 2017;155:159–68.
13. Schmidt P, Gaser C, Arsic M, et al. An automated tool for detection of FLAIR-hyperintense white-matter lesions in Multiple Sclerosis. *NeuroImage* 2012;59(4):3774–83.
14. Kuhlmann T, Ludwin S, Prat A, Antel J, Brück W, Lassmann H. An updated histological classification system for multiple sclerosis lesions. *Acta Neuropathol* (Berl) 2017;133(1):13–24.
15. Bankhead P, Loughrey MB, Fernández JA, et al. QuPath: Open source software for digital pathology image analysis. *Sci Rep* 2017;7(1):16878.
16. DeLuca GC. The contribution of demyelination to axonal loss in multiple sclerosis. *Brain* 2006;129(6):1507–16.
17. Diaz-Sanchez M, Williams K, DeLuca GC, Esiri MM. Protein co-expression with axonal injury in multiple sclerosis plaques. *Acta Neuropathol* (Berl) 2006;111(4):289–99.
18. Hillert J, Stawiarz L. The Swedish MS registry – clinical support tool and scientific resource. *Acta Neurol Scand* 2015;132(S199):11–9.
19. Manouchehrinia A, Stridh P, Khademi M, et al. Plasma neurofilament light levels are associated with risk of disability in multiple sclerosis. *Neurology* 2020;94(23):e2457–67.
20. Huang J, Khademi M, Fugger L, et al. Inflammation-related plasma and CSF biomarkers for multiple sclerosis. *Proc Natl Acad Sci* 2020;117(23):12952–60.
21. McCaw ZR, Lane JM, Saxena R, Redline S, Lin X. Operating characteristics of the rank-based inverse normal transformation for quantitative trait analysis in genome-wide association studies. *Biometrics* 2020;76(4):1262–72.
22. Benkert P, Meier S, Schaedelin S, et al. Serum neurofilament light chain for individual prognostication of disease activity in people with multiple sclerosis: a retrospective modelling and validation study. *Lancet Neurol* 2022;21(3):246–57.
23. Havrdova E, Galetta S, Stefoski D, Comi G. Freedom from disease activity in multiple sclerosis. *Neurology* 2010;74(Issue 17, Supplement 3):S3–7.